Coupled Capillary Wave Fluctuations in Thin Aqueous Films on an Aqueous Subphase

Ming Li,[1] Aleksey M. Tikhonov,[1] David J. Chaiko,[2] and Mark L. Schlossman[1,3,*]

[1]*Department of Physics, University of Illinois, 845 W. Taylor Street, Chicago, Illinois 60607*
[2]*Chemical Technology Division, Argonne National Laboratory, 9700 S. Cass Avenue, Argonne, Illinois 60439*
[3]*Department of Chemistry, University of Illinois, 845 W. Taylor Street, Chicago, Illinois 60607*

(Received 27 November 2000)

X-ray scattering and interfacial tension measurements are used to demonstrate the formation of nanometer-thick aqueous films on aqueous bulk subphases from polymer-salt biphase mixtures. X-ray scattering determines a coupling constant that characterizes the coupled capillary wave fluctuations of the liquid-vapor and liquid-liquid interfaces of this thin film. These data also determine an effective Hamakar constant that characterizes the long-range interaction between the interfaces and parameters that characterize the short-range part of the interfacial interaction.

DOI: 10.1103/PhysRevLett.86.5934 PACS numbers: 68.15.+e, 61.10.Eq, 68.05.–n, 82.65.+r

Wetting phenomena at interfaces are very sensitive to the form of the potential that governs the interaction between the interfaces. For example, x-ray scattering studies of thin wetting films on solid substrates have shown that thermal fluctuations of the liquid surface are reduced by the long-range van der Waals interaction from the substrate [1]. Studies of these thin films are useful for understanding the role of short- and long-range forces in interfacial statistical physics.

We chose to study thin aqueous liquid films on top of bulk aqueous liquid subphases for several reasons. First, aqueous biphase systems are used, for example, for the purification and separation of biological materials [2]. We anticipate that these thin films may be of use for biophysical studies and have used them to study ordering in a protein monolayer at the liquid-liquid interface (to be published). Second, the interfacial free energy potential that characterizes this wetting phenomenon is between two liquid interfaces, the liquid-vapor interface and the liquid-liquid interface. Numerous x-ray scattering measurements have demonstrated the suitability of capillary wave theory to describe the fluctuations of a single liquid interface. When two liquid interfaces are placed in close proximity, the interfacial potential creates a coupling between the capillary fluctuations. This coupling can be simply described by a perturbative modification of the capillary wave Hamiltonian. This allows us to determine the curvature near the minimum of the interfacial potential. By assuming a simple form for the interfacial potential we can also derive parameters that characterize the long- and short-range interactions between the interfaces.

We studied biphase mixtures of polyethylene glycol [PEG; $H(OCH_2CH_2)_nOH$, $Mn = 3400$, from Aldrich], potassium phosphate (K_2HPO_4 from Fluka, 99.5%), and Barnstead Nanopure water [2]. The mixtures were shaken, equilibrated for 20+ hours at room temperature, and the two phases separated (the top PEG-rich phase is denoted PEG* and the bottom salt-rich phase is denoted salt*). The interfacial tension between the two phases, $\gamma_{\mathrm{salt}^*/\mathrm{PEG}^*} \equiv \gamma_2 = 7.0 \pm 0.5$ mN/m, and the surface tensions of each phase with air, $\gamma_{\mathrm{PEG}^*/\mathrm{air}} \equiv \gamma_1 = 51.6 \pm 0.2$ mN/m and $\gamma_{\mathrm{salt}^*/\mathrm{air}} = 77.2 \pm 0.2$ mN/m, were measured by the drop-weight and Wilhelmy plate methods, respectively.

X-ray reflectivity and off-specular diffuse scattering measurements were performed on beam line X19C at the National Synchrotron Light Source (Brookhaven National Laboratory), as described elsewhere [3]. A vapor-tight Teflon sample cell with a circular trough for the liquid sample and a water reservoir to maintain the humidity was temperature controlled at 35.0 ± 0.03 °C (these results are not sensitive to small changes in temperature). The sample was prepared by placing a small drop of the top phase onto the bottom phase surface. The drop spreads and thins rapidly, as is evident from the rapidly changing optical interference pattern that spreads across the surface. After a few seconds the thin layer becomes unstable and forms an irregular pattern, which then collapses to form small lenses in about 1 h. A pipette is used to mechanically move the lenses out of the x-ray beam path. The macroscopic lenses function as reservoirs for the thin film PEG* top phase. Although spontaneous formation of an equilibrium thin film from the lower phase might be expected, the thin film was not observed unless a drop was added. The following results are independent of the precise volume of the initial drop.

Figure 1 shows an example of R/R_F, the specular reflectivity normalized by the Fresnel reflectivity (for an ideal smooth and flat interface), as a function of the wave vector transfer normal to the interface Q_z [for specular reflection $\beta = \alpha$, $Q_x = Q_y = 0$, and $Q_z = (4\pi/\lambda)\sin\alpha$, where $\lambda = 0.825$ Å]. The oscillations in the reflectivity are due to interference between x rays reflected from the top and bottom of the layer. The decay of the oscillations in R/R_F can be modeled by the presence of different interfacial widths at the liquid-vapor and liquid-liquid interfaces (for comparison, the dashed line in Fig. 1 is the best fit with identical interfacial widths). The solid line is a fit from a

 0031-9007/01/86(26)/5934(4)$15.00

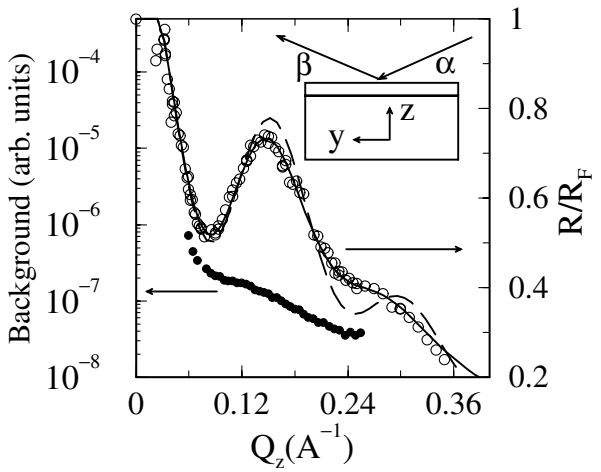

FIG. 1. Specular reflectivity intensity normalized to the Fresnel reflectivity, R/R_F (open circles). Fits described in the text. Off-specular background scattering intensities (solid dots). Inset: Thin film x-ray scattering geometry.

standard Born approximation analysis using a single layer model [3,4]. This analysis yields the layer thickness $l_m = 40.2 \pm 0.3$ Å (the peak at $Q_z \approx 0.15$ Å^{-1} corresponds to $2\pi/Q_z \approx l_m$), the liquid-liquid interfacial width $\sigma_2 = 7.9 \pm 0.3$ Å, the liquid-vapor width $\sigma_1 = 2.9 \pm 0.2$ Å, and the electron density of the film relative to the subphase, $\rho_{e,\mathrm{film}}/\rho_{e,\mathrm{sub}} = 0.84 \pm 0.02$ [5]. The width $\sigma_2 \gg \sigma_1$ because the tension $\gamma_2 \ll \gamma_1$. We expect $\sigma \propto \sqrt{1/\gamma}$, therefore $\sigma_2/\sigma_1 \approx \sqrt{\gamma_1/\gamma_2}$, in agreement with our measurements. Our measurements indicate that the layer is a thin film of a PEG-rich solution rather than just a monolayer of PEG molecules adsorbed to the interface. A monolayer of PEG has a measured thickness of 10 Å, less than the thickness of our film [6]. Also, the radius of gyration of our PEG under similar conditions has been measured to be close to 10 Å, also less than the film thickness [7].

Figure 1 also shows the background (diffuse) scattering intensities measured off the specular condition by averaging intensity values at wave vector transfer $\mathbf{Q} = (0, +\Delta Q_y, Q_z)$, and $\mathbf{Q} = (0, -\Delta Q_y, Q_z)$ [3]. Correlations between the heights of neighboring interfaces will produce peaks in the diffuse scattering at values of Q_z corresponding to maxima in the specular reflectivity [8]. As seen in Fig. 1, weak oscillations are visible in the background that mimic those in R/R_F.

For a quantitative analysis of the coupling of the capillary wave fluctuations between the two interfaces, we chose to measure off-specular diffuse scattering from the interfaces by scanning β for fixed $\alpha = 0.56°$ and $\alpha = 0.75°$, as shown in Fig. 2. Off-specular diffuse scattering data from single liquid interfaces roughened by thermal capillary wave fluctuations have been previously described by the distorted wave Born approximation (DWBA) [9,10]. The interfacial roughness is characterized by the height-height correlation function, defined as $C(\mathbf{r}) = \langle \zeta(0)\zeta(\mathbf{r})\rangle$, where $\zeta(\mathbf{r})$ is the local interfacial height of a sharp interface above the mean interfacial plane, and $\mathbf{r}$ is the displacement between two points on the interface. The correlation function is determined by an analysis of the capillary wave Hamiltonian [11]. In this model, the interfacial widths previously mentioned are the result of capillary wave roughening of a sharp interface. The range in Q space of our data does not justify the use of more complicated models of the interface [12]. Here, we modify the standard capillary wave Hamiltonian to account for the interfacial coupling, derive the correlation functions, and compute the off-specular diffuse scattering from the DWBA.

Modification of the Hamiltonian proceeds from the observation that the equilibrium thickness of the film corresponds to a minimum in the interfacial potential, or excess free energy of the wetting film, ΔG. This occurs at the point l_m (see Fig. 3) at which $\partial \Delta G/\partial l = 0$. We expand $\Delta G(l)$ near the minimum to second order, $\Delta G(l) = -C + \frac{1}{2}B(l - l_m)^2$, to get the coupling constant B between the two interfaces. Adding the energy of the thermal fluctuations to the free energy, one has the Hamiltonian of the system, per unit area [13,14],

$$H = \frac{1}{A_0}\int d^2r \left\{ \sum_{i=1,2} [\gamma_i(1 + \tfrac{1}{2}\zeta_{ix}^2 + \tfrac{1}{2}\zeta_{iy}^2) + \tfrac{1}{2}g\Delta\rho_{mi}\zeta_i^2] + \tfrac{1}{2}B(\zeta_1 - \zeta_2)^2 \right\}$$
$$= \sum_{i=1,2}\left\{ \gamma_i + \sum_q \tfrac{1}{2}(B + g\Delta\rho_{mi} + \gamma_i q^2)\alpha_i(q)\alpha_i(-q) \right\} - \tfrac{1}{2}B\sum_q [\alpha_1(q)\alpha_2(-q) + \alpha_1(-q)\alpha_2(q)], \quad (1)$$

where A_0 is the interfacial area, $i = 1, 2$ refers to the PEG*-air interface and salt*-PEG* interface, respectively, ζ_{ix} is the x derivative of ζ_i, g is the gravitational acceleration, and $\Delta\rho_{mi}$ is the difference in mass density across interface i. The upper equation is the standard capillary wave Hamiltonian [11] with the addition of the term proportional to B that represents a local coupling of the positions of the two interfaces. A theoretical treatment of coupled capillary waves that goes beyond this Gaussian approximation has been discussed in the literature [15]. The lower equation is a representation in reciprocal space, where $\alpha(q)$ is the Fourier transform of $\zeta(\mathbf{r})$ [$= \sum_q \alpha(q)\exp(i\mathbf{q}\cdot\mathbf{r})$, where $\mathbf{q}$ is the in-plane capillary wave vector]. The canonical average of the correlation functions in reciprocal space is given by

$$\langle \alpha_k(q)\alpha_l(-q)\rangle = \frac{2}{A_0}\frac{k_B T X_{kl}}{4M_1M_2 - B^2}, \quad (2)$$

where $X_{11} = M_2$, $X_{22} = M_1$, $X_{12} = B$, k_B is Boltzmann's constant, T is the temperature, and $M_i = B/2 + g\Delta\rho_{mi}/2 + \gamma_i q^2/2$, $i = 1, 2$. The Fourier transforms of Eq. (2) are the height-height correlation functions of the

individual interfaces, $C_{11}(\mathbf{r})$, $C_{22}(\mathbf{r})$, and the height-height cross-correlation function between the two interfaces, $C_{12}(\mathbf{r})$. As expected, as $B \to 0$ the cross-correlation function $C_{12}(\mathbf{r}) \to 0$. As $B \to \infty$ the three correlation functions become identical, indicating complete conformality between the interfacial fluctuations.

The first order DWBA expression for scattering from two interfaces can be approximated for our system to yield the intensity of diffuse scattering [12,16–18],

$$I_{\mathrm{diff}} = \frac{I_0}{\sin\alpha}\frac{Q_c^4}{256\pi^2}\int d\beta\, d\phi |T(\alpha)|^2|T(\beta)|^2 \times \left\{\sum_{j=1,2}\left[\Delta\rho_j^2\frac{e^{-\sigma_j^2\,\mathrm{Re}(Q_z^t)^2}}{|Q_z^t|^2}\int (e^{|Q_z^t|^2 C_{jj}(\mathbf{r})} - 1)e^{i\mathbf{Q}_{xy}\mathbf{r}}\, d^2\mathbf{r}\right] + 2\Delta\rho_1\Delta\rho_2\cos(Q_z l_m)\frac{e^{(-1/2)(\sigma_1^2+\sigma_2^2)\,\mathrm{Re}(Q_z^t)^2}}{|Q_z^t|^2}\int (e^{|Q_z^t|^2 C_{12}(\mathbf{r})} - 1)e^{i\mathbf{Q}_{xy}\mathbf{r}}\, d^2\mathbf{r}\right\}, \quad (3)$$

where I_0 is incident intensity, Q_c is the wave vector for total reflection, $T(\alpha)$ and $T(\beta)$ are the Fresnel transmission coefficients, $\Delta\rho_j$ is the difference in electron density across each interface, and Q_z^t is the z component of the momentum transfer with respect to the lower phase. Integration over β and ϕ corresponds to the angular acceptance range of the detector. The two incident angles chosen for the measurements correspond to nearly minimum ($Q_z = 0.20$ Å^{-1}) and maximum values ($Q_z = 0.15$ Å^{-1}) for the $\cos(Q_z l_m)$ term, thus providing greater sensitivity to the cross-correlation function in Eq. (3).

The data at both incident angles in Fig. 2 are fit simultaneously using Eq. (3) combined with the standard expression for the reflectivity from the DWBA [10]. Two parameters are fit, the coupling B and a small constant background (independent of β) that represents scattering from the bulk liquid. The analysis yields $B = 1.4^{+1.6}_{-0.8} \times 10^{11}$ J/m^4 (1σ error bars, 2σ errors are $B = 1.4^{+5.0}_{-1.0} \times 10^{11}$ J/m^4). The solid lines in Fig. 2 show the best fit value; dashed lines show the fit for $B = 0$ and $B = 10^{20}$ J/m^4 for comparison.

It is interesting to compare our measured value of the coupling constant B to a coupling constant B_H previously derived for interacting tensionless membranes whose fluctuations are determined by the membrane's bending modulus κ rather than the interfacial tension as in our system. The Helfrich Hamiltonian leads to $B_H = 36k_BT^2/(\pi^2\kappa l^4)$, which yields $B_H = 1.4 \times 10^{12}$ J/m^4 for flexible membranes with $\kappa \approx k_BT$ or $B_H = 3.4 \times 10^{10}$ J/m^4 for a rigid liquid crystalline membrane with $\kappa \approx 40k_BT$ [19]. The coupling in our system lies between these values for the coupling within a stack of either flexible or rigid tensionless membranes.

Our measurement of B can also be compared to a compression modulus measured for freely suspended soap films that span the range from 10^{11} to 10^{14} J/m^4, depending upon composition [8]. This indicates that the coupling of interfacial fluctuations in soap films is either similar to or greater than in our thin film.

A model for the free energy F (per unit area) of this film of thickness l is $F(l) = \gamma_2 + \gamma_1 + \Delta G(l)$ [20]. For large l, $\Delta G(l)$ tends to zero. The interfacial potential $\Delta G(l)$ includes a repulsive short-range force and an attractive long-range van der Waals interaction, written as [21]

$$\Delta G(l) = S_p \exp[(l_0 - l)/\Lambda] - A/12\pi l^2, \quad (4)$$

where S_p is the amplitude of the short-range interaction, A is an effective Hamakar constant, and l_0 sets the distance for the hard core repulsion [21]. The first term in Eq. (4) models a short-range interaction with decay length Λ, and

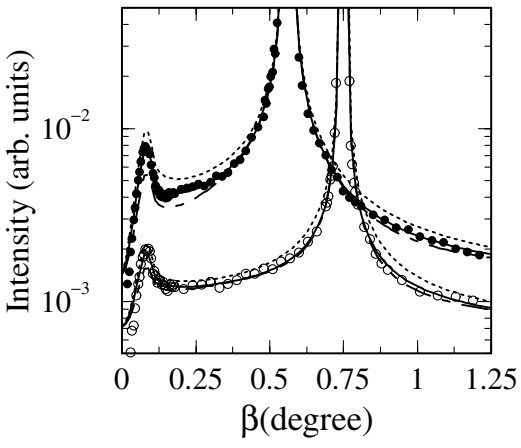

FIG. 2. Off-specular diffuse scattering at $\alpha = 0.56°$ (solid dots) and $\alpha = 0.75°$ (open circles). Fits are to $B = 1.4 \times 10^{11}$ J/m^4 (solid line), $B = 0$ (short dashed line), and $B = 10^{20}$ J/m^4 (long dashed line).

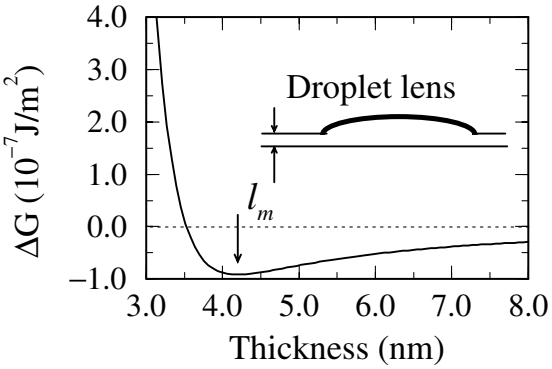

FIG. 3. Interfacial potential, $\Delta G(l)$, given in Eq. (4) with parameters given in the text. Inset: Macroscopic lens in equilibrium with a film of thickness l_m (not to scale).

the second term is the van der Waals interaction between two planar interfaces separated by a distance l. It has been shown that this model can account for many features of wetting films, including the incomplete wetting that occurs in our system [20,21].

Three parameters in Eq. (4) are determined by the following conditions and by choosing $l_0 = 1.57$ Å [21], though the parameters are insensitive (within the stated accuracy) to the range $1 < l_0 < 3$ Å. (i) $\Delta G(l \to l_0) = S$, where the spreading coefficient $S = \gamma_{\mathrm{salt}^*/\mathrm{air}} - (\gamma_2 + \gamma_1) = 18.6$ mN/m is given by our macroscopic measurements of the tensions [20]. (ii) At the minimum of the interfacial potential, $\partial \Delta G(l_m)/\partial l = 0$ and $\partial^2 \Delta G(l_m)/\partial l^2 = B$, where l_m is given by the fit to the reflectivity data, and B is given by the fit to the diffuse scattering data. These conditions yield $\Lambda = 2.9 \pm 0.2$ Å, $S_p = 18.7 \pm 0.5$ mN/m, and the Hamakar constant $A = 8^{+10}_{-5} \times 10^{-23}$ J. The excess free energy given by Eq. (4) with these parameters is plotted in Fig. 3. The decay length Λ is similar to the close-packed distances of these molecules. It is expected that mutual hindrance of capillary waves leads to an effective entropic repulsion between the interfaces, which is exponential [15], though other short-range interactions may also contribute to this decay length. As discussed by Brochard-Wyart *et al.* [20], the sign of the Hamakar constant and the spreading coefficient are consistent with our observation of macroscopic drops in equilibrium with a very thin layer that covers the interface (see inset, Fig. 3), though we have chosen a different sign convention for the effective Hamakar constant than in Ref. [20]. The effective Hamakar constant is the difference between two Hamakar constants, $A = A_{\mathrm{PEG}^*,\mathrm{PEG}^*} - A_{\mathrm{PEG}^*,\mathrm{salt}^*}$. A is small ($A \approx k_B T/50$), indicating that the attraction of the upper phase to the lower phase is only slightly different from the attraction of the upper phase to itself.

In summary, we formed nanometer-thick aqueous films supported on an aqueous subphase and have shown that x-ray scattering probes the coupled interfacial fluctuations in these films. A perturbative, local modification of the standard capillary wave Hamiltonian allowed us to determine a coupling constant for these interfaces. Combining the x-ray measurements with macroscopic measurements of the interfacial tensions allowed us to determine the parameters in a model free energy for the thin film. These included the Hamakar constant describing the long-range interactions and the decay length and amplitude of the short-range interactions.

We observed similar wetting phenomena with a larger molecular weight PEG and by polyvinylpyrrolidone substituted for the PEG. It is likely that these thin partial wetting films are common in aqueous biphase systems. The techniques presented here may prove useful for probing interactions across small regions of aqueous phases.

M. L. S. is supported by the Chemical Technology Division at Argonne National Laboratory and NSF DMR. Brookhaven National Laboratory is supported by the DOE.

*Email address: schloss@uic.edu

[1] I. M. Tidswell *et al.,* Phys. Rev. Lett. **66**, 2108 (1991); A. K. Doerr *et al.,* Phys. Rev. Lett. **83**, 3470 (1999); J. Wang *et al.,* Phys. Rev. Lett. **83**, 564 (1999).

[2] B. Y. Zaslavsky, *Aqueous Two-Phase Partitioning* (Marcel Dekker, New York, 1995).

[3] M. L. Schlossman *et al.,* Rev. Sci. Instrum. **68**, 4372 (1997).

[4] M. L. Schlossman and P. S. Pershan, in *Light Scattering by Liquid Surfaces and Complementary Techniques,* edited by D. Langevin (Marcel Dekker, New York, 1992), p. 365.

[5] Compositions were determined from phase diagrams [2]. Top phase: 65.8% ± 0.5% PEG, 2.0% ± 0.5% salt, 32.2% ± 0.5% water; bottom phase: 0.5% ± 0.5% PEG, 34.4% ± 0.5% salt, 65.1% ± 0.5% water. Compositions and measured mass densities (bottom phase, 1.38 g/cm^3; top phase, 1.11 g/cm^3), yield electron densities (bottom phase, 4.44×10^{23}/cm^3; top phase, 3.64×10^{23}/cm^3). The relative electron density ($3.64/4.44 = 0.82 \pm 0.02$) agrees with the x-ray measurement.

[6] J. A. Benderson *et al.,* Macromolecules **26**, 4591 (1993).

[7] P. Thiyagarajan, D. J. Chaiko, and R. P. Hjelm, Macromolecules **28**, 7730 (1995).

[8] J. Daillant and O. Belorgey, J. Chem. Phys. **97**, 5824 (1992); **97**, 5837 (1992); S. K. Sinha *et al.,* Physica (Amsterdam) **198B**, 72 (1994), and references therein.

[9] D. K. Schwartz *et al.,* Phys. Rev. A **41**, 5687 (1990).

[10] S. K. Sinha *et al.,* Phys. Rev. B **38**, 2297 (1988).

[11] F. P. Buff, R. A. Lovett, and F. H. Stillinger, Phys. Rev. Lett. **15**, 621 (1965).

[12] S. Dietrich and A. Haase, Phys. Rep. **260**, 1 (1995).

[13] J. S. Rowlinson and B. Widom, *Molecular Theory of Capillarity* (Clarendon, Oxford, 1982); B. V. Derjaguin, N. V. Charaev, and V. M. Muller, *Surface Forces* (Consultants Bureau, New York, 1987); M. O. Robbins, D. Andelman, and J.-F. Joanny, Phys. Rev. A **43**, 4344 (1991).

[14] M. L. Schlossman *et al.,* in *Applications of Synchrotron Radiation Techniques to Materials Science V,* edited by S. R. Stock (Materials Research Society, Warrendale, 2000), p. 165.

[15] S. Dietrich, M. P. Nightingale, and M. Schick, Phys. Rev. B **32**, 3182 (1985).

[16] V. Holy *et al.,* Phys. Rev. B **47**, 15 896 (1993); V. Holy and T. Baumbach, Phys. Rev. B **49**, 10 668 (1994).

[17] J. Stettner *et al.,* Phys. Rev. B **53**, 1398 (1996).

[18] Equation (3) is a good approximation to the first order DWBA for our system because (1) for most of the data, $\alpha, \beta > 3\alpha_c$ (angle for total reflection $\alpha_c \approx 0.08°$) and Eq. (3) reduces to the Born approximation, correct for this angular range; (2) $\alpha \gg \alpha_c$; (3) in the notation of Ref. [17], $q^0_{z,1} \approx q^1_{z,1}$; (4) the film is very thin, so $|T(\alpha, \beta)|^2 \approx |T_3|^2$ (see [17]); and (5) $(q_z \sigma_1)^2 \ll 1$.

[19] W. Helfrich, Z. Naturforsch. **33A**, 305 (1978); S. A. Safran, *Statistical Thermodynamics of Surfaces, Interfaces, and Membranes* (Addison Wesley, Reading, 1994).

[20] P. G. de Gennes, Rev. Mod. Phys. **57**, 827 (1985); F. Brochard-Wyart *et al.,* Langmuir **7**, 335 (1991).

[21] A. Sharma and R. Khanna, Phys. Rev. Lett. **81**, 3463 (1998); C. J. van Oss, *Interfacial Forces in Aqueous Media* (Marcel Dekker, New York, 1994).